Monitoring the pH Dependence of IR Carboxylic Acid Signals upon Q_B^- Formation in the Glu-L212 → Asp/Asp-L213 → Glu Swap Mutant Reaction Center from *Rhodobacter sphaeroides*†

Eliane Nabedryk,*,‡,§ Mark L. Paddock,|| Melvin Y. Okamura,|| and Jacques Breton§

Service de Bioénergetique, CEA-Saclay, 91191 Gif-sur-Yvette Cedex, France, and Department of Physics, University of California, San Diego, La Jolla, California 92093

Received September 21, 2006; Revised Manuscript Received November 24, 2006

ABSTRACT: In the photosynthetic reaction center (RC) from the purple bacterium *Rhodobacter sphaeroides*, proton-coupled electron-transfer reactions occur at the secondary quinone (Q_B) site. Involved in the proton uptake steps are carboxylic acids, which have characteristic infrared vibrations in the 1770−1700 cm^{-1} spectral range that are sensitive to $^1H/^2H$ isotopic exchange. With respect to the native RC, a novel protonation pattern for carboxylic acids upon Q_B photoreduction has been identified in the Glu-L212 → Asp/Asp-L213 → Glu mutant RC using light-induced FTIR difference spectroscopy (Nabedryk, E., Breton, J., Okamura, M. Y., and Paddock, M. L. (2004) *Biochemistry 43*, 7236−7243). These carboxylic acids are structurally close and have been implicated in proton transfer to reduced Q_B. In this work, we extend previous studies by measuring the pH dependence of the Q_B^-/Q_B FTIR difference spectra of the mutant in ^1H_2O and ^2H_2O. Large pH dependent changes were observed in the 1770−1700 cm^{-1} spectral range between pH 8 and pH 4. The IR fingerprints of the protonating carboxylic acids upon Q_B^- formation were obtained from the calculated double-difference spectra ^1H_2O minus ^2H_2O. These IR fingerprints are specific for each pH, indicative of the contribution of different titrating groups. In particular, the 1752 cm^{-1} signal indicates that Glu-L213 protonates upon Q_B^- formation at pH ≥ 5, whereas the 1746 cm^{-1} signal indicates protonation of Asp-L212 even at pH 4. An unidentified carboxylic acid absorbing at ∼1765 cm^{-1} could be the proton donor between pH 8 and 5. The observation that in the swap mutant there are several uniquely behaving carboxylic acids shows that electrostatic interactions occurring between them are sufficiently modified from the native RC to reveal their IR signatures.

In the reaction center from the photosynthetic purple bacterium *Rhodobacter sphaeroides*, light energy is rapidly converted to chemical energy through coupled electron−proton transfer to a buried quinone molecule Q_B[1]. Light-induced electron transfer is initiated from the primary electron donor (a dimer of bacteriochlorophyll) through a series of electron acceptors to the loosely bound quinone Q_B (ubiquinone-10). The double reduction of Q_B to quinol (Q_BH_2) takes place in a multistep process and requires the transfer of two electrons coupled to the uptake of two protons from the solution (*1*). Kinetic studies of site-directed RC mutants (*1*−*3*), together with a number of electrostatic calculations (*4*−*13*) based on the available structural data (*14*−*17*), have emphasized specific roles for several polar and acid residues forming a cluster near Q_B (*16*, *18*). In particular, Ser-L223, Asp-L213, and Glu-L212 (Figure 1) were shown to be crucial for rapid coupled electron−proton transfer to reduced Q_B (*1*−*3*).

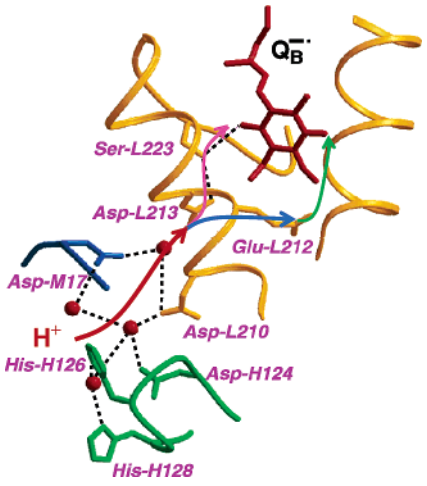

FIGURE 1: Structure of the reaction center from *Rb. sphaeroides* near the secondary quinone Q_B (from PDB ID code 1AIG (*16*)). The arrows represent the general proton flow from the surface near His-H126 and His-H128 to reduced Q_B via Asp-L213 and Glu-L212. The proton transfer between carboxylic acids (labeled in the Figure) along the pathway is the topic of this article. The red spheres represent bound water molecules.

† This work was supported by NIH Grant GM 41637 to M.Y.O.

‡ This work is dedicated to Eliane Nabedryk's grandsons Adrien and Antoine.

* To whom correspondence should be addressed. Phone: 331 69087112. Fax: 331 69088717. E-mail: eliane.nabedryk@cea.fr.

§ CEA-Saclay.

|| University of California, San Diego.

[1] Abbreviations: RC, reaction center; P, primary electron donor; H_B, bacteriopheophytin cofactor; Q_A, primary quinone electron acceptor; Q_B, secondary quinone electron acceptor.

10.1021/bi0619627 CCC: $37.00
Published on Web 01/09/2007

The first electron transfer to Q_B results in substoichiometric proton binding by the RC protein, revealing a change of the pK_a of amino acid side chains between the states Q_B and Q_B^- (*19*−*21*). Involved in the proton uptake steps are carboxylic acids that have characteristic infrared vibrations that are observable using light-induced FTIR difference spectroscopy. Bands arising from the C═O stretching mode of protonated side chains of Asp and Glu are found in a clear region of the IR spectrum between 1770 and 1700 cm^{-1} and are sensitive to $^1H/^2H$ isotopic exchange (*22*). The earliest experiments showed that when Q_B^- is formed in native RCs, substoichiometric protonation of a carboxylic acid occurs at pH 7 (*23*, *24*), resulting in a single IR signal at 1728 cm^{-1}. The 1728 cm^{-1} band was absent in all of the RC mutants lacking Glu-L212 (*23*−*28*), whereas it remained in a number of RC carboxylic mutants at the various sites (Asp-L210, Asp-M17, Glu-H173, Asp-L213) (*23*, *26*, *27*, *29*) located less than ∼10 Å from Q_B (Figure 1). Thus, the 1728 cm^{-1} signal was assigned to the protonation of Glu-L212 upon Q_B^- formation. However, despite the abundance of carboxylic acids forming a cluster located structurally in the vicinity of Q_B, and the expected strong electrostatic interactions between them (*5*, *6*, *16*, *18*), no significant IR signal (sensitive to $^1H/^2H$ isotopic exchange) attributable to another carboxylic acid could be identified in the Q_B^-/Q_B spectra of the native or of any of those mutant RCs (*23*−*27*, *29*). This is also in contrast to expectation from a number of electrostatic computational work (*5*−*7*, *10*, *13*). In general, there is no consensus between experimental and theoretical work on the protonation states of the two key residues Asp-L213 and Glu-L212 in the Q_B neutral state and on the IR extent of proton uptake by these residues upon Q_B^- formation. Most of the electrostatic calculations predict that a cluster of acids composed of Asp-L210, Asp-L213, and Glu-L212, exhibiting non-classic titration behavior, share one proton in the Q_B state and two protons in the Q_B^- state, although the exact location of the protons is still controversial (*4*−*13*).

Recently, a novel strategy was developed to probe new protonation patterns of internal carboxylic acids in the bacterial RC from *Rb. sphaeroides*. This was accomplished by changing the microscopic electrostatic environment near Q_B without perturbing the overall macroscopic environment, that is, by switching Asp and Glu at the L212 and L213 sites, respectively (*30*). Kinetic measurements on the Glu-L212 → Asp/Asp-L213 → Glu swap mutant RC suggested that the overall electrostatic environment near Q_B was similar to that of the native RC, but there was a difference in the microscopic electrostatic environment attributed to differences in the state of ionization of Asp and Glu at either L212 or L213 (*30*).

The strategy to interchanging Asp and Glu at L212 and L213 (i.e., Glu-L212 → Asp/Asp-L213 → Glu) resulted in the observation of novel protonation patterns of carboxylic acids upon Q_B^- formation (*28*); henceforth, we will abbreviate the name of the mutant as the swap mutant. The Q_B^-/Q_B FTIR spectrum at pH 7 of the swap mutant RC in the 1770−1700 cm^{-1} range shows several distinct new signals that are sensitive to $^1H/^2H$ isotopic exchange, indicating that the reduction of Q_B results in the change of protonation state and/or environment of several carboxylic acids (*28*). Compared with the single prominent positive peak observed at 1728 cm^{-1} in the native RC (*23*), a broad positive band at 1752−1747 cm^{-1} was revealed in the Q_B^-/Q_B spectrum of the swap mutant, together with a positive signal at 1731 cm^{-1} and a new broad negative feature at 1765 cm^{-1}. The broad band at 1752−1747 cm^{-1} was tentatively assigned to an increase of protonation in response to Q_B reduction of Glu-L213 (at 1752 cm^{-1}) and Asp-L212 (at 1747 cm^{-1}), on the basis of the effect of replacing these residues with their amine analogues (*28*). These results show that the protonation patterns of carboxylic acids and, hence, their resultant FTIR signatures are very sensitive to the environment and can be strongly affected by what is often considered fairly conservative amino acid replacements (Asp with Glu and Glu with Asp). It was concluded that the swap mutations at L212 and L213 influence a cluster of carboxylic acids larger than the L212/L213 acid pair. Although proton sharing among a carboxylic acid cluster in the native RC has been predicted from electrostatic calculations (*4*−*13*), it is only in the swap RC that it has been experimentally evidenced, i.e., there are sufficient differences that reveal the IR signatures of the individual components (*28*). Understanding the different behavior between the native RC and the swap mutant is important for elucidating proton-transfer reactions within the bacterial RC and key to reconciling experimental and computational results. More generally, the protonation state of acidic and basic residues and their changes upon redox reactions is important for the understanding of the proton-coupled electron-transfer mechanisms in membrane−protein complexes of the respiratory and photosynthetic chains (e.g., cytochrome oxidase, cytochrome bc_1).

In the present work, we have investigated the pH dependence of the Q_B^-/Q_B light-induced FTIR difference spectra of the Asp-L212/Glu-L213 swap mutant, in particular the pH effects on the IR signals of protonated carboxylic acid groups. When individual titrable groups interact with each other, for example, in a cluster of polar and acid residues, their pH dependence can be much more complex than that of an individual group. Here, pH is used to help deconvolute the spectra. The relative contribution of individual groups to the FITR spectra is weighted by the intrinsic pK_a of the carboxylic acids and the pH of the measurement. Large pH dependent changes were observed in the 1770−1700 cm^{-1} absorption range of the Q_B^-/Q_B FTIR difference spectrum of the Asp-L212/Glu-L213 swap mutant at pH values ranging from 8 to 4. Thus, the novel protonation pattern of carboxylic acids previously identified in the swap mutant (*28*) was also found to be strongly pH-dependent.

EXPERIMENTAL PROCEDURES

The construction of the site-directed mutant Asp-L212/Glu-L213 was previously described (*30*, *31*). RCs were isolated in *N*,*N*′-dimethyldodecylamine *N*-oxide (LDAO) as previously described (*32*). A detailed description of the preparation of RC samples for FTIR experiments has been given (*23*, *33*). The Q_B site was reconstituted with Q_{10} by adding an ∼10-fold excess of Q_{10}. The RC samples were prepared in different buffers: 100 mM Tris-HCl at pH 8 and 100 mM sodium acetate at pH 5 and pH 4. The Q_B^- state was generated in the presence of potassium ferrocyanide (250 mM) and *N*,*N*,*N*′,*N*′-tetramethyl-*p*-phenylenediamine (TMPD) (50 mM) as previously described (*34*) with single saturating flash excitation (Nd:YAG laser, 7 ns, 530 nm) (*23*, *33*). The preparation of RC samples in ^2H_2O was carried

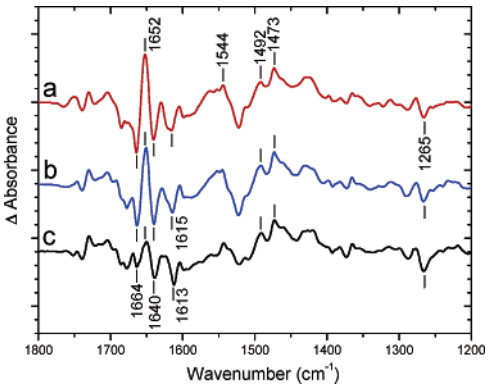

FIGURE 2: Light-induced Q_B^-/Q_B FTIR difference spectra of the Asp-L212/Glu-L213 swap mutant RC from *Rb. sphaeroides* in ^1H_2O at pH 8 (a), pH 5 (b), and pH 4 (c). Between 100 000 and 200 000 interferograms were averaged. The frequency of the peaks is given at ±1 cm^{-1}. The minor tick marks on the vertical axis are separated by 10^{-4} absorbance units.

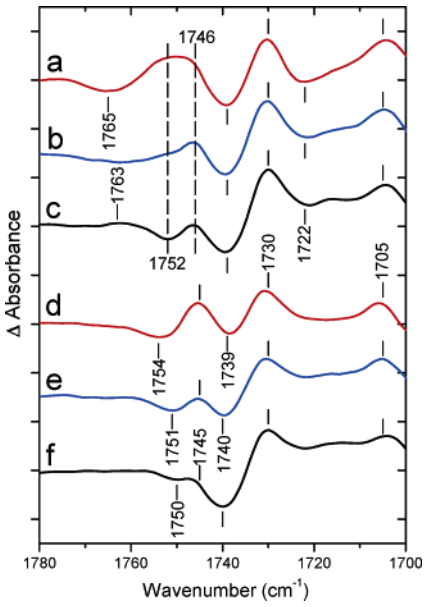

FIGURE 3: Comparison of the 1780−1700 cm^{-1} spectral region of the Q_B^-/Q_B spectra of the Asp-L212/Glu-L213 mutant RC from *Rb. sphaeroides* in ^1H_2O at pH 8 (a), pH 5 (b), and pH 4 (c) and in ^2H_2O at pD 8 (d), pD 5 (e), and pD 4 (f). The marks on the vertical axis are separated by 10^{-4} absorbance units.

out as previously reported (*29*), using deuterated buffers (>90% ^2H) and a mixture of potassium ferrocyanide and TMPD prepared in ^2H_2O. The ^2H_2O procedure leads to the deuteration of about 70% NH peptide groups.

Steady-state light-induced FTIR difference spectra of the Q_B to Q_B^- transition in mutant RCs were recorded at 10 °C in ^1H_2O or ^2H_2O, with a Nicolet 60SX spectrometer equipped with a MCT-A detector and a KBr beam-splitter, as previously described (*23*, *33*). Difference Q_B^-/Q_B spectra were calculated from each of the 16 or 32 scans (acquisition time 3 or 6 s) recorded before and after single-turnover laser flash excitation. Blocks of spectra were stored every hour, allowing comparison of the spectra recorded at early time to those obtained at later times. For each of the ^1H_2O and ^2H_2O samples at a given pH (pD), the successive blocks of spectra were found to be reproducible for at least ∼30 h and were, therefore, averaged. Moreover, final spectra represent an average of 3−6 samples. Spectral resolution was 4 cm^{-1}.

RESULTS

Overall Description of the Q_B^-/Q_B FTIR Spectra of the Asp-L212/Glu-L213 Swap Mutant RC at Different pH Values. Figure 2 shows the Q_B^-/Q_B light-induced FTIR difference spectra in the 1800−1200 cm^{-1} range of the Asp-L212/Glu-L213 mutant RCs measured at pH 8, pH 5, and pH 4 in ^1H_2O. The Q_B^-/Q_B spectrum obtained at pH 8 (Figure 2a) was very similar to the one previously reported at pH 7 (*28*). In contrast, the Q_B^-/Q_B spectra obtained at pH 5 (Figure 2b) and pH 4 (Figure 2c) show several large differences, as detailed below.

In all Q_B^-/Q_B spectra, positive bands result from signals present in the Q_B^- state, whereas negative bands results from the loss of signals present in the neutral Q_B state. As previously reported (*33*, *35*, *36*), vibrational bands from the neutral quinone Q_B are expected in the 1660−1600 cm^{-1} spectral range, whereas the semiquinone Q_B^- modes lie in the 1500−1400 cm^{-1} range. In the swap mutant RC (*28*), C═O and C═C modes of Q_B contribute at 1640 and ∼1615 cm^{-1}, respectively (Figure 2), as also observed in native RCs (*33*, *35*, *36*). In comparison to a single anion band peaking at 1479 cm^{-1} in the Q_B^-/Q_B spectrum of native RCs (*23*, *33*), two distinct signals appeared at 1492 and 1473 cm^{-1} in the Q_B^-/Q_B spectrum of the swap mutant (Figure 2). Note that the neutral and anion modes of the secondary quinone of the swap mutant were not pH sensitive.

The protein contributions (backbone and side chains) are found in the ∼1700−1600 cm^{-1} (amide I) and 1570−1520 cm^{-1} (amide II) ranges. The intensity of the protein signals in the 1700−1640 cm^{-1} region, notably at 1664 (−), 1652 (+), and 1640 (−) cm^{-1} was only slightly decreased at pH 5 compared to that at pH 8, but it was largely decreased at pH 4. In the present work, the 1570−1520 cm^{-1} region probably also contains contributions from $TMPD^+$/TMPD modes, which explains the differences observed in the amide II region between the spectra previously obtained at pH 7 in the presence of diaminodurene (*28*) and the one shown here at pH 8 (Figure 2a). In a pure $TMPD^+$/TMPD difference spectrum (Breton, J., unpublished data), the main IR signal was observed at 1546 (+)/1520 (−) cm^{-1}, with minor contributions at 1618 (−), 1430 (+), 1382 (+), and 1365 (−) cm^{-1}. The protonated side chains of Asp and Glu carboxylic acids contribute at 1770−1700 cm^{-1} (*22*, *37*, *38*). No signals from $TMPD^+$/TMPD are expected in this range. Because the protonation signals are of particular interest, we will present them separately below.

pH Dependent Changes of the 1780−1700 cm^{-1} region of the Q_B^-/Q_B FTIR Spectra of the Asp-L212/Glu-L213 Swap Mutant. Figure 3 shows the 1780−1700 cm^{-1} region of the Q_B^-/Q_B spectra of the Asp-L212/Glu-L213 swap mutant at pH 8, pH 5, and pH 4 in ^1H_2O (a−c) and in ^2H_2O (d−f). The signals observed in the protonated carboxylic acid region of the swap mutant at pH 8 (Figure 3a and d) were identical to those previously described at pH 7 in ^1H_2O and ^2H_2O (*28*). In ^1H_2O, the spectra at pH 8 and pH 7 both showed a negative feature at 1765 cm^{-1} (−), a broad positive band centered at around 1750 cm^{-1}, a negative signal at 1739 cm^{-1}, and two positive peaks at 1730 and 1705 cm^{-1}. The pattern of this region was remarkably different from that found in the native RC at pH 7 (*23*) or pH 8 (*26*), where a single prominent

positive peak was seen at 1728 cm^{-1}. In ^2H_2O, the spectra of the swap mutant at pD 8 (Figure 3d) and pD 7 (*28*) also displayed the same peaks with a negative feature at 1754 cm^{-1} (−), a positive band at 1745 cm^{-1}, a negative signal at 1739 cm^{-1}, and two positive peaks at 1730 and 1705 cm^{-1}.

Figure 3 shows that the novel protonation pattern observed in the swap mutant was pH-dependent. The largest differences occur in the 1780−1740 cm^{-1} range, where the broad, positive signal observed at the highest frequency range was affected. As the pH was lowered from pH 8 to 5 in ^1H_2O, the amplitude of the absorption of the highest frequency component at around 1752 cm^{-1} decreased, revealing more clearly the peak at 1746 cm^{-1} (compare Figure 3a and b). Decreasing the pH to 4 (Figure 3c) resulted in the appearance of a broad, positive feature at ∼1763 cm^{-1}, a negative signal at 1752 cm^{-1}, and a considerable decrease of the 1746 cm^{-1} signal. In contrast, the positive peaks at 1730 and 1705 cm^{-1} as well as the trough at 1739 cm^{-1} were present at all pH values.

In ^2H_2O, there are pH dependent changes, although the details differed slightly. Decreasing pD from 8 to 5 (Figure 3d and e) resulted in a negative band at 1751 cm^{-1}, and the amplitude of the positive band at 1745 cm^{-1} was considerably reduced with respect to the large signal observed at pD 8. Decreasing pD to 4 (Figure 3f) induced additional shifts and/or amplitude changes of peaks in the 1780−1740 cm^{-1} range, notably at 1750, 1745, and 1740 cm^{-1}.

Thus, several of the bands seen in the FTIR difference spectra presented in Figure 3 show dissimilar sensitivity to both pH and $^1H/^2H$ isotopic exchange. The simplest to interpret were those due to distinct isolated signals. For example, at pH 8, the negative feature at 1765 cm^{-1} observed in ^1H_2O was downshifted to 1754 cm^{-1} in ^2H_2O. The Q_B^-/Q_B spectra (Figure 3) clearly showed that the underlying components of the broad band centered at 1750 cm^{-1} (Figure 3a) have different pH sensitivities. This difference induced a decrease of the highest frequency component (at around 1752 cm^{-1}) at pH 5 (Figure 3b), whereas the lowest frequency component (at around 1746 cm^{-1}) was present at this pH. However, for most of the carboxylic signals of the 1760−1720 cm^{-1} region, band shifts and amplitude changes resulting from the $^1H/^2H$ isotopic exchange and pH changes, respectively, lead to overlapping signal changes, making it difficult to unambiguously deconvolute the behavior of the individual components.

The specific effects of pH on the protonation pattern of the carboxylic acids in the Q_B^-/Q_B spectum of the swap mutant are best visualized in the double-difference spectra calculated from the individual Q_B^-/Q_B spectra recorded at a given pH (pH 8, 5, and 4) in ^1H_2O and in ^2H_2O. In such double-difference spectra (^1H_2O minus ^2H_2O), each carboxylic acid whose protonation state changes upon Q_B^- formation is expected to contribute a single derivative signal composed of a positive peak next to a negative trough downshifted by ∼5−10 cm^{-1}. Figure 4 shows the calculated double-difference spectra ^1H_2O minus ^2H_2O at pH 8 (a), pH 5 (b), and pH 4 (c). Apart from a common feature present in all spectra at 1730(+)/∼1722 (−) cm^{-1}, the calculated spectra reveal several distinct features. These differences demonstrated that at each pH, a unique combination of carboxylic acids contributed to the observed spectra.

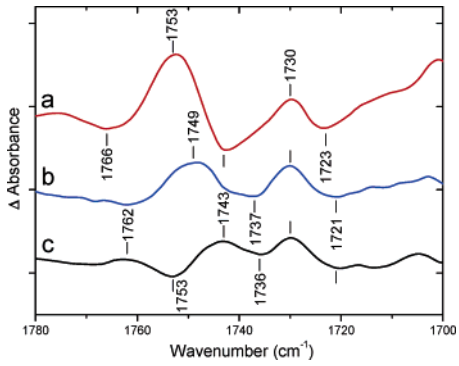

FIGURE 4: Comparison of the calculated double-difference spectra ^1H_2O minus ^2H_2O for the Asp-L212/Glu-L213 mutant RC from *Rb. sphaeroides* at pH 8 (a), pH 5 (b), and pH 4 (c). Each division on the vertical scale corresponds to 10^{-4} absorbance units.

The observed spectra showed a convolution of contributions with the superposition of several bandshifts. The richness of the observed spectra made unambiguous assignments difficult at this stage; therefore, just the main features are summarized below. The main feature of the double-difference spectrum ^1H_2O minus ^2H_2O calculated at pH 8 (Figure 4a) was a positive peak at 1753 cm^{-1} and a negative band at 1743 cm^{-1}. At pH 5 (Figure 4b), the double-difference spectrum showed a broad, positive band at 1749 cm^{-1} and a broad trough between 1743 and 1737 cm^{-1}. At pH 4 (Figure 4c), a negative signal appeared at 1753 cm^{-1} and a positive one at 1743 cm^{-1}. The shift of the broad band around 1770−1760 cm^{-1} differed at each pH, displaying a negative component at 1766 cm^{-1} at pH 8, almost featureless at pH 5, and displaying a positive, broad feature at 1762 cm^{-1} at pH 4. If all carboxylic groups involved in the Q_B to Q_B^- formation had the same titration pattern with pH, the double-difference spectra ^1H_2O minus ^2H_2O obtained at each pH would be identical. Hence, the differences in the spectra at each pH indicate that they result from the superposition of peaks from titrating groups having different titration behaviors.

DISCUSSION

IR difference spectroscopy is a very sensitive tool to detect changes in the protonation state of carboxylic acid side chains. In this study, we investigated the protonation of internal carboxylic acids in a mutant RC from *Rb. sphaeroides* in response to Q_B reduction using FTIR difference spectroscopy as a function of pH. We studied a swap mutant that had Asp at L212 and Glu at L213; the native one has Glu at L212 and Asp at L213. The carboxylic acid region of the swap mutant showed several new bands appearing in response to Q_B reduction. The sensitivity of these bands to $^1H/^2H$ exchange showed that they correspond to the protonation of internal acids. In a previous report, possible assignments for these new carboxylic acid signals were investigated by studying two additional double mutant RCs combining either Asp-L212 with Gln-L213 or Asn-L212 with Glu-L213. In this article, the strategy used to investigate this novel protonation pattern was to study the pH dependence of Q_B^-/Q_B FTIR difference spectra of the Asp-L212/Glu-L213 swap mutant in ^1H_2O and ^2H_2O. Upon Q_B^- formation, the change of the protonation state of a given carboxylic acid (referred to as ΔH^+ in the text) is determined by its

change of pK_a between the Q_B and the Q_B^- states[2]. Large pH-dependent changes of proton uptake were observed in the pH range 8 to 4.

pH Dependence of the Proton Uptake (ΔH^+) of Carboxylic Acids Involved in the Q_B to Q_B^- Reaction. The effect of pH and of $^1H/^2H$ exchange on the Q_B^-/Q_B spectra of the swap mutant revealed that at least three different carboxylic acids were involved in changes of protonation or environment upon Q_B reduction. Three carboxylic acids result in the ~1765, 1752, and 1746 cm^{-1} signals in ^1H_2O (Figure 3). A possible fourth resulted in the 1730(+)/~1722(−) cm^{-1} signal common to all of the double-difference spectra ^1H_2O minus ^2H_2O (Figure 4). The ^1H_2O minus ^2H_2O IR fingerprint spectra demonstrated that the pH dependence of ΔH^+ differed for the two main components of the broad band centered at 1750 cm^{-1} as well as for the small signal at ~1765 cm^{-1} (Figure 4). The highest frequency component near 1752 cm^{-1} was assigned to the ΔH^+ of an isolated carboxylic acid that occurs at pH 8 and pH 5 but not at pH 4. The lowest frequency component near 1746 cm^{-1} corresponded to the ΔH^+ of a different carboxylic acid occurring over the entire pH range from 8 to 4. At pH 4, the absorption at 1746 cm^{-1} was very small. Thus, the IR data demonstrated that the protonation of the 1752 cm^{-1} component occurred at pH ≥ 5, whereas that of the 1746 cm^{-1} component occurred even at pH 4.

Where do these two components appear in ^2H_2O? Taking into account the spectra in both Figures 3 and 4, we propose that the 1752 cm^{-1} component (Figure 3a) downshifted to ~1745 cm^{-1} in ^2H_2O (Figure 3d), whereas the 1746 cm^{-1} component (Figure 3a) shifted to ~1739 (+) cm^{-1} (Figure 3d) because the trough at 1739 cm^{-1} appears less negative in ^2H_2O (Figure 3d) than in ^1H_2O (Figure 3a). This proposal was supported by the data shown in Figure 4, notably at pH 5, that showed a broad, positive peak at ~1749 cm^{-1} and a broad trough lying between 1743 and 1737 cm^{-1}, which could account (in part) for the shift of the 1746 cm^{-1} component. Note that such frequency downshifts by 5−10 cm^{-1} from ^1H_2O to ^2H_2O are typical for protonated carboxylic groups (*22*, *37*, *38*).

The negative feature observed at ~1765 cm^{-1} at pH 8 (Figure 3a) and the positive signal appearing at ~1763 cm^{-1} at pH 4 (Figure 3c) could reflect either a pH-dependent environmental change of a protonated carboxylic acid or ΔH^+ of a carboxylic acid, with ΔH^+ approaching zero at pH 5 (Figure 3b). The 2 cm^{-1} frequency shift that is observed between pH 8 and pH 4 could result from local electrostatic changes. These signals are also clearly identified in the double-difference spectra ^1H_2O minus ^2H_2O (Figure 4) at pH 8 (negative signal at 1766 cm^{-1}) and pH 4 (positive signal at 1762 cm^{-1}).

We discuss below possible assignments in comparison with previous data obtained on the corresponding amine analogues of the swap mutant (*28*).

Assignments of pH-Dependent Signals to Glu-L213 and Asp-L212: Comparison with the Swap Amine Analogues. The contributions of Glu-L213 and Asp-L212 in the swap mutant have been previously investigated by comparing the Q_B^-/Q_B spectra of the swap mutant at pH 7 in ^1H_2O and ^2H_2O with those of the Asn-L212/Glu-L213 and Asp-L212/Gln-L213 mutant RCs (*28*). The broad band centered at 1750 cm^{-1} in the swap mutant was tentatively assigned to an increase in protonation upon Q_B^- formation of the two side chains Glu-L213 at 1752 cm^{-1} and Asp-L212 at 1747 cm^{-1}. Indeed, the present pH-dependent study of the Q_B reduction in the swap mutant demonstrates that the two main signals previously identified at 1752 and 1747[3] cm^{-1} responded differently to a change of pH from pH 8 to pH 4. Thus, the present data strengthen the previous tentative assignments and further demonstrate that the protonation of Glu-L213 occurs at pH ≥ 5, whereas the protonation of Asp-L212 occurs even at pH 4. Note that the protonation pattern observed at pH 10 for the swap mutant (Nabedryk, E. et al., unpublished data) was similar to the one observed at pH 8, indicating p$K_a(Q_B^-)$ >10. Thus, the titrating acids have significant interactions (>3pK_a units, 180 meV) with Q_B^-, implying that they must be located nearby (<7 Å for a dielectric constant of 15).

Because the changes observed at ~1765 cm^{-1} are small in amplitude, they could arise from an acid located further from Q_B; this results in a smaller signal (ΔH^+) due to a smaller interaction with Q_B^-. Also, because the protonation state of this acid decreased upon Q_B^- formation (i.e., it decreased its pK_a), it is likely located between the closest groups and the surface. Because the 1770−1760 cm^{-1} region is flat at pH 7 in the FTIR spectrum of the mutant RC with Asn at L212 and Glu at L213 (*28*), the negative signal observed at 1765 cm^{-1} in the swap mutant could be the proton donor to Asp-L212. Possible carboxylic acids that are located between the surface of the RC protein and the destination of the protons near L212 and L213 are Asp-L210, Asp-M17, and Glu-H173 (Figure 1). In native RCs, Asp-L210 was suggested to be involved in the Q_B to Q_B^- reaction by electrostatic computations (*5*, *6*) and time-resolved FTIR measurements (*39*); Asp-M17 had a synergistic effect on net proton flow through the pathways (*40*); and Glu-H173 electrostatically influenced other groups in the pathway (*41*, *42*), in particular Q_B^- and Glu-L212. Although all possibly contributing to the signal, further studies involving additional mutations at L210, M17, and H173 in the swap mutant RC background will be necessary to determine the relative contributions of these carboxylic acids to the ~1765 cm^{-1} signal.

The 1730(+)/~1722(−) cm^{-1} signal was common to all of the double-difference spectra ^1H_2O minus ^2H_2O obtained at pH 8, 5, and 4 (Figure 4). Approximately one-third of the 1730 cm^{-1} peak titrated; the remaining two-third was invariant (Figure 3). The invariant, positive signal at 1730 cm^{-1} can be associated with the 1739 cm^{-1} negative signal, which was insensitive to $^1H/^2H$ isotope exchange (Figure 3): these two signals are not assigned to a perturbation of a carboxylic acid but could account for an electrochromic shift of the 10a-ester C═O IR mode of H_B, as previously suggested (*23*, *43*).

[2] For the simple case of two interacting groups, ΔH^+ has a peak at a pH that is the average of its p$K_a(Q_B)$ and p$K_a(Q_B^-)$. At pH values significantly below p$K_a(Q_B)$ or above p$K_a(Q_B^-)$, ΔH^+ is null, and no FTIR signal corresponding to the protonation of carboxylic side chains is observed.

[3] In the present work, the pH effect on the Q_B^-/Q_B spectra indicates that the lowest frequency component that is assigned to Asp-L212 peaks at 1746 cm^{-1}.

Comparison with the Native RC: Single Carboxylic Acid Titration versus Multiple Acid Titration in the Swap Mutant. For all of the pH values investigated, the spectra of the swap mutant RC displayed large differences with respect to that of the native RC. In the protonated carboxylic acid region from 1780 to 1700 cm^{-1}, the Q_B^-/Q_B spectrum of the native RC at pH 7 or 8 showed only a single positive prominent band at 1728 cm^{-1}, which was assigned to substoichiometric proton uptake by Glu-L212 upon Q_B reduction (*23*−*27*). Consistent with this assignment, this band was absent in mutant RCs in which Glu was absent at L212, i.e., in RCs with Gln at L212 (*23*−*27*) and in RCs with Asp at L212 (swap mutant RC) or Asn at L212 (*28*). Furthermore, the protonated carboxylic acid region of the Q_B^-/Q_B spectrum of native RCs displayed a similar ^1H_2O minus ^2H_2O IR fingerprint pattern at pH 8 (*26*), pH 7 (*23*), and pH 4 (Nabedryk, E., and Breton, J., unpublished data). Such similar IR fingerprints observed for the carboxylic acid(s) in the native RC upon Q_B^- formation at different pH values indicate the involvement of the same titrating group(s) over the whole pH range investigated. These observations contrast the large differences observed in the 1780−1700 cm^{-1} absorption range of the Q_B^-/Q_B spectrum of the swap mutant RC between pH 8 and 4. Therefore, the Q_B^-/Q_B spectra of the native RC and the swap mutant are not only very different in their protonation patterns but also very different in their pH-dependences.

Why are the native and the swap mutant different? FTIR spectra at different pH values of the swap mutant are rich in information on the behavior of internal carboxylic acids. The observation of several distinct carboxylic bands in the swap mutant indicated that protonation or proton movement occurred among several carboxylic acids upon Q_B^- formation. The present observation that these carboxylic bands were differentially sensitive to pH changes showed that electrostatic interactions occurring between these acids, in particular, those at L212 and L213 sites, were different from those occurring in the native RC. Differences in the electrostatic interactions among the acids of the cluster near Q_B resulting from the interchange of Glu for Asp at L212 and Asp for Glu at L213 could be a possible cause for the changes in the FTIR spectra. In this regard, electrostatic calculations of the interactions of carboxylic acids near Q_B in the swap mutant should help to establish the differences in interactions and, hence, the resultant FTIR spectrum; this is a nontrivial and challenging exercise, given the number of titrating groups in close proximity and the unknown positions of many internal water molecules (*16*, *18*). In addition, an attractive approach would be to use time-resolved FTIR spectroscopy (*39*) to follow the protonation changes of individual carboxylic groups at different pH values. Such an approach should provide detailed information on the molecular mechanism of electron and proton transfer during Q_B photoreduction.

Could a Water Molecule Play a Role in the Proton Transfer in the Native RC? An interesting possible explanation for the differences between the native and mutant RC is that an internal water molecule may be a proton acceptor in the native system (in addition to Glu-L212). Protonation of an internal water molecule was indicated on the basis of electrostatic computations (*44*) and FTIR measurements (*45*−*47*) in bacteriorhodopsin, a different type of photosynthetic protein that pumps protons across a bacterial membrane. The protonated water was located between two carboxylic acid groups on the exit pathway. In the bacterial RC, there is a region located between three carboxylic acid groups, that is, Asp-L210, Asp-L213, and Asp-M17 (Figure 1), which could accommodate for the location of water molecules. The idea that internal water molecules in the vicinity may protonate was supported by earlier FTIR measurements in which the polarizable proton IR continuum, possibly due to the protonation of internal water molecules (*48*), were perturbed by mutations near Q_B (*49*). Although the results are not as definitive as those for bacteriorhodopsin, the protonation of internal water molecules in the native RC can qualitatively explain the differences observed here between the native and mutant RCs upon Q_B reduction. Testing such a proposal provides a new challenge for FTIR difference spectroscopy.

REFERENCES

1. Paddock, M. L., Feher, G., and Okamura, M. Y. (2003) Proton transfer pathways and mechanism in bacterial reaction centers, *FEBS Lett. 555*, 45−50.
2. Okamura, M. Y., Paddock, M. L., Graige, M. S., and Feher, G. (2000) Proton and electron transfer in bacterial reaction centers, *Biochim. Biophys. Acta 1458*, 148−163.
3. Wraight, C. A. (2004) Proton and electron transfer in the acceptor quinone complex of photosynthetic reaction centers from *Rhodobacter sphaeroides*, *Front. Biosci. 9*, 309−337.
4. Gunner, M. R., and Honig, B. (1992) Calculations of Proton Uptake in *Rhodobacter sphaeroides* Reaction Centers, in *The Photosynthetic Bacterial Reaction Center II* (Breton, J., and Verméglio, A., Eds.) pp 403−410, Plenum Press, New York.
5. Beroza, P., Fredkin, D. R., Okamura, M. Y., and Feher, G. (1995) Electrostatic calculations of amino acid titration and electron transfer, $Q_A^-Q_B \rightarrow Q_AQ_B^-$, in the reaction center, *Biophys. J. 68*, 2233−2250.
6. Alexov, E. G., and Gunner, M. R. (1999) Calculated protein and proton motions coupled to electron transfer: Electron transfer from Q_A^- to Q_B in bacterial photosynthetic reaction centers, *Biochemistry 38*, 8253−8270.
7. Grafton, A. K., and Wheeler, R. A. (1999) Amino acid protonation states determine binding sites of the secondary ubiquinone and its anion in the *Rhodobacter sphaeroides* photosynthetic reaction center, *J. Phys. Chem. B 103*, 5380−5387.
8. Rabenstein, B., Ullmann, G. M., and Knapp, E.-W. (2000) Electron transfer between the quinones in the photosynthetic reaction center and its coupling to conformational changes, *Biochemistry 39*, 10487−10496.
9. Walden, S. E., and Wheeler, R. A. (2002) Protein conformational gate controlling binding site preference and migration for ubiquinone-B in the photosynthetic reaction center of *Rhodobacter sphaeroides*, *J. Phys. Chem. B 106*, 3001−3006.
10. Ishikita, H., Morra, G., and Knapp, E.-W. (2003) Redox potential of quinones in photosynthetic reaction centers from *Rhodobacter sphaeroides*: Dependence on protonation of Glu-L212 and Asp-L213, *Biochemistry 42*, 3882−3892.
11. Taly, A., Sebban, P., Smith, J. C., and Ullmann, G. M. (2003) The position of Q_B in the photosynthetic reaction center depends on pH: A theoretical analysis of the proton uptake upon Q_B reduction, *Biophys. J. 84*, 2090−2098.
12. Ishikita, H., and Knapp, E-W. (2004) Variation of Ser-L223 hydrogen bonding with the Q_B redox state in reaction centers from *Rhodobacter sphaeroides*, *J. Am. Chem. Soc. 126*, 8059−8064.
13. Zhu, Z., and Gunner, M. R. (2005) Energetics of quinone-dependent electron and proton transfers in *Rhodobacter sphaeroides* photosynthetic reaction centers, *Biochemistry 1*, 82−96.
14. Allen, J. P., Feher, G., Yeates, T. O., Komiya, H., and Rees, D. C. (1988) Structure of the reaction center from *Rhodobacter sphaeroides* R-26: Protein-cofactor (quinones and Fe^{2+}) interactions, *Proc. Natl. Acad. Sci. U.S.A. 85*, 8487−8491.
15. Ermler, U., Fritzsch, G., Buchanan, S. K., and Michel, H. (1994) Structure of the photosynthetic reaction centre from *Rhodobacter*

sphaeroides at 2.65 Å resolution: cofactors and protein-cofactor interactions, *Structure 2*, 925−936.
16. Stowell, M. H. B., McPhillips, T. M., Rees, D. C., Soltis, S. M., Abresch, E., and Feher, G. (1997) Light-induced structural changes in photosynthetic reaction center: Implications for mechanism of electron-proton transfer, *Science 276*, 812−816.
17. Camara-Artigas, A., Brune, D., and Allen, J. P. (2002) Interactions between lipids and bacterial reaction centers determined by protein crystallography, *Proc. Natl. Acad. Sci. U.S.A. 99*, 11055−11060.
18. Abresch, E. C., Paddock, M. L., Stowell, M. H. B., McPhillips, T. M., Axelrod, H. L., Soltis, S. M., Rees, D. C., Okamura, M. Y., and Feher, G. (1998) Identification of proton transfer pathways in the X-ray structure of the bacterial reaction center from *Rhodobacter sphaeroides*, *Photosynth. Res. 55*, 119−125.
19. Maróti, P., and Wraight, C. A. (1988) Flash-induced H^+ binding by bacterial photosynthetic reaction centers: Influences of the redox states of the acceptor quinones and primary donor, *Biochim. Biophys. Acta 934*, 329−347.
20. McPherson, P. H., Okamura, M. Y., and Feher, G. (1988) Light-induced proton uptake by photosynthetic reaction centers from *Rhodobacter sphaeroides* R-26. I. Protonation of the one-electron states $D^+Q_A^-$, DQ_A^-, $D^+Q_AQ_B^-$, and $DQ_AQ_B^-$, *Biochim. Biophys. Acta 934*, 348−368.
21. Miksovska, J., Schiffer, M., Hanson, D. K., and Sebban, P. (1999) Proton uptake by bacterial reaction centers: the protein complex responds in a similar manner to the reduction of either quinone acceptor, *Proc. Natl. Acad. Sci. U.S.A. 96*, 14348−14353.
22. Rich, P. R., and Iwaki, M. (2005) Infrared Spectroscopy as a Tool to Study Protonation Reactions within Proteins, in *Biophysical and Structural Aspects of Bioenergetics* (Wikstrom, M., Ed.) Chapter 13, pp 314−333, Royal Society of Chemistry, Cambridge, England.
23. Nabedryk, E., Breton, J., Hienerwadel, R., Fogel, C., Mäntele, W., Paddock, M. L., and Okamura, M. Y. (1995) Fourier transform infrared difference spectroscopy of secondary quinone acceptor photoreduction in proton transfer mutants of *Rhodobacter sphaeroides*, *Biochemistry 34*, 14722−14732.
24. Hienerwadel, R., Grzybek, S., Fogel, C., Kreutz, W., Okamura, M. Y., Paddock, M. L., Breton, J., Nabedryk, E., and Mäntele, W. (1995) Protonation of Glu-L212 following Q_B^- formation in the photosynthetic reaction center of *Rhodobacter sphaeroides*: Evidence from time-resolved infrared spectroscopy, *Biochemistry 34*, 2832−2843.
25. Nabedryk, E., Breton, J., Joshi, H. M., and Hanson, D. K. (2000) Fourier transform infrared evidence of proton uptake by glutamate L212 upon reduction of the secondary quinone Q_B in the photosynthetic reaction center from *Rhodobacter capsulatus*, *Biochemistry 39*, 14654−14663.
26. Nabedryk, E., Breton, J., Okamura, M. Y., and Paddock, M. L. (2001) Simultaneous replacement of Asp-L210 and Asp-M17 with Asn increases proton uptake by Glu-L212 upon first electron transfer to Q_B in reaction centers from *Rhodobacter sphaeroides*, *Biochemistry 40*, 13826−13832.
27. Mezzetti, A., Nabedryk, E., Breton, J., Okamura, M. Y., Paddock, M. P., Giacometti, G., and Leibl, W. (2002) Rapid-scan Fourier transform infrared spectroscopy shows coupling of Glu-L212 protonation and electron transfer to Q_B in *Rhodobacter sphaeroides* reaction centers, *Biochim. Biophys. Acta 1553*, 320−330.
28. Nabedryk, E., Breton, J., Okamura, M. Y., and Paddock, M. L. (2004) Identification of a novel protonation pattern for carboxylic acids upon Q_B photoreduction in *Rhodobacter sphaeroides* reaction center mutants at Asp-L213 and Glu-L212 sites, *Biochemistry 43*, 7236−7243.
29. Nabedryk, E., Breton, J., Okamura, M. Y., and Paddock, M. L. (1998) Proton uptake by carboxylic groups upon photoreduction of the secondary quinone (Q_B) in bacterial reaction centers from *Rhodobacter sphaeroides*: FTIR studies on the effects of replacing Glu H173, *Biochemistry 37*, 14457−14462.
30. Paddock, M. L., Feher, G., and Okamura, M. Y. (1997) Proton and electron transfer to the secondary quinone (Q_B) in bacterial reaction centers: The effect of interchanging the electrostatics in the vicinity of Q_B by interchanging Asp and Glu at the L212 and L213 sites, *Biochemistry 36*, 14238−14249.
31. Paddock, M. L., Rongey, S. H., McPherson, P. H., Juth, A., Feher, G., and Okamura, M. Y. (1994) Pathway of proton transfer in bacterial reaction centers: Role of aspartate-L213 in proton transfers associated with reduction of quinone to hydroquinone, *Biochemistry 33*, 734−745.
32. Paddock, M. L., Rongey, S. H., Abresch, E. C., Feher, G., and Okamura, M. Y. (1988) Reaction centers from three herbicide resistant mutants of *Rhodobacter sphaeroides* 2.4.1: Sequence analysis and preliminary characterization, *Photosynth. Res. 17*, 75−96.
33. Breton, J., Boullais, C., Berger, G., Mioskowski, C., and Nabedryk, E. (1995) Binding-sites of quinones in photosynthetic bacterial reaction centers investigated by light-induced FTIR difference spectroscopy: Symmetry of the carbonyl interactions and close equivalence of the Q_B vibrations in *Rhodobacter sphaeroides* and *Rhodopseudomonas viridis* probed by isotope labeling, *Biochemistry 34*, 11606−11616.
34. Breton, J., Wakeham, M. C., Fyfe, P. K., Jones, M. R. and Nabedryk, E. (2004) Characterization of bonding interactions of Q_B upon photoreduction via A-branch or B-branch electron transfer in mutant reaction centers from *Rhodobacter sphaeroides*, *Biochim. Biophys. Acta 1656*, 127−138.
35. Brudler, R., de Groot, H. J. M., van Liemt, W. B. S., Gast, P., Hoff, A. J., Lugtenburg, J., and Gerwert, K. (1995) FTIR spectroscopy shows weak symmetric hydrogen bonding of the Q_B carbonyl groups in *Rhodobacter sphaeroides* R26 reaction centers, *FEBS Lett. 370*, 88−92.
36. Breton, J., and Nabedryk, E. (1996) Protein-quinone interactions in the bacterial photosynthetic reaction center: Light-induced FTIR difference spectroscopy of the quinone vibrations, *Biochim. Biophys. Acta 1275*, 84−90.
37. Venyaminov, S. Yu., and Kalnin, N. N. (1990) Quantitative IR spectrophotometry of peptide compounds in water (H_2O) solutions. I. Spectral parameters of amino acid residue absorption bands, *Biopolymers 30*, 1243−1257.
38. Rahmelow, K., Hübner, W., and Ackermann, Th. (1998) Infrared absorbance of protein side chains, *Anal. Biochem. 257*, 1−11.
39. Rémy, A., and Gerwert, K. (2003) Coupling of light-induced electron transfer to ptoton uptake in photosynthesis, *Nat. Struct. Biol. 10*, 637−644.
40. Paddock, M. L., Ädelroth, P., Chang, C., Abresch, E. C., Feher, G., and Okamura, M. Y. (2001) Identification of the proton pathway in bacterial reaction centers: Cooperation between Asp-M17 and Asp-L210 facilitates proton transfer to the secondary quinone (Q_B), *Biochemistry 40*, 6893−6902.
41. Takahashi, E., and Wraight, C. A. (1996) Potentiation of proton transfer function by electrostatic interactions in photosynthetic reaction centers from *Rhodobacter sphaeroides*: First results from site-directed mutation of the H subunit, *Proc. Natl. Acad. Sci. U.S.A. 93*, 2640−2645.
42. Ishikita, H., and Knapp, E.-W. (2005) Energetics of proton transfer pathways in reaction centers from *Rhodobacter sphaeroides*, *J. Biol. Chem. 280*, 12446−12450.
43. Breton, J., Bibikova, M., Oesterhelt, D., and Nabedryk, E. (1998) Electrostatic Influence of Q_A or Q_B Reduction on the 10a-Ester C═O Vibration of H_A in *Rp. viridis*, in *Photosynthesis: Mechanisms and Effects* (Garab, G., Ed.) Vol. 2, pp 687−692, Kluwer Academic Publishers, Dordrecht, The Netherlands.
44. Spassov, V. Z., Lueke, H., Gerwert, K., and Bashford, D. (2001) pK(a) Calculations suggest storage of an excess proton in a hydrogen-bonded water network in bacteriorhodopsin, *J. Mol. Biol. 312*, 203−19.
45. Garczarek, F., Wang, J., El-Sayed, M. A., and Gerwert, K. (2004) The assignment of the different infrared continuum absorbance changes observed in the 3000−1800 cm^{-1} region during the bacteriorhodopsin photocycle, *Biophys. J. 87*, 2676−2682.
46. Garczarek, F., Brown, L. S., Lanyi, J. K., Gerwert, K. (2005) Proton binding within a membrane protein by a protonated water cluster, *Proc. Natl. Acad. Sci. U.S.A. 102*, 3633−3638.
47. Garczarek, F., and Gerwert, K. (2006) Functional waters in intraprotein proton transfer monitored by FTIR difference spectroscopy, *Nature 439*, 109−112.
48. Breton, J., and Nabedryk, E. (1998) Proton uptake upon quinone reduction in bacterial reaction centers: IR signature and possible participation of a highly polarizable hydrogen bond network, *Photosynth. Res. 55*, 301−307.
49. Nabedryk, E., Okamura, M. Y., Paddock, M. L., and Breton, J. (2002) Perturbation of the polarizable proton infrared continuum upon Q_B reduction in mutant reaction centers from *Rb. sphaeroides. Biophys. J. 82*, 197a.

BI0619627